River Flow 2010 - Dittrich, Koll, Aberle & Geisenhainer (eds) - © 2010 Bundesanstalt für Wasserbau ISBN 978-3-939230-00-7

An innovative methodology/technology for streamflow observation

K. Kawanisi, M. Razaz & S. Watanabe
Department of Civil and Environmental Engineering, Graduate School of Engineering, Hiroshima University, 1-4-1 Kagamiyama, Higashi Hiroshima, Japan

A. Kaneko
Department of Ocean Atmosphere Environment Laboratory, Graduate School of Engineering, Hiroshima University, 1-4-1 Kagamiyama, Higashi Hiroshima, Japan

T. Abe
Ministry of Land, Infrastructure, Transport and Tourism, 3-20 Nakaku Hachoubori, Hiroshima, Japan

ABSTRACT: Long-term variations of stream flow and salinity in a tidal river were measured by an innovative technology, called the Fluvial Acoustic Tomography (FAT). The reciprocal sound transmission was performed between two acoustic stations located on both sides of the river. The FAT system makes a breakthrough with the following aspects: (a) accurate time with GPS clock signals, (b) high signal-to-noise ratio with 10^{th} order M-sequence modulation, (c) low power consumption, small and lightweight. Even for the tidal rivers with periodic intrusion of salt wedge, streamwise cross-sectional average velocity estimated from the travel time difference data were in good agreement with the average velocity observed by an array of moored downward-looking ADCPs. The measurement of flow rate was carried out successfully even in flood events with high SSC and large ambient noise levels of sound. The flow rate of FAT system also agreed well with the results of ADCPs and float observations during the flood events. As well, cross-sectional average salinity was estimated using the sound speed determined from the reciprocal sound transmission and the mean temperature measured by temperature sensors.

Keywords: Acoustic tomography, Discharge, Saltwater intrusion, Flood flow, Tidal estuary

1 INTRODUCTION

River discharge is an important hydrological factor in river and coastal planning/management, control of water resources, and environment conservation. Therefore, it is a key issue to establish a reliable measurement method and associated technology for measuring stream flow with high accuracy. However, it is very difficult to measure the cross-sectional average velocity in unsteady flows or during extreme hydrological events like floods.

Often, river discharge is estimated indirectly from water level or velocity near water surface. However, these methods have only limited applications.

For continuous measurement of water discharge, just a few different equipments are available, e.g., acoustic velocity meters (AVMs), horizontal acoustic Doppler current profilers (H-ADCPs), etc. (Catherine & DeRose, 2004; Wang & Huang, 2005). The main drawback of previous methods is that the number of velocity sample points in cross-section of stream is often insufficient to estimate the cross-sectional average velocity. H-ADCPs can measure horizontal profile of velocity in a range with sufficient strength of acoustical backscatter. However, H-ADCPs do not provide any information about vertical velocity profiles. Moreover, their profile range decreases with increasing SSC (Suspended Sediment Concentration). In addition, the H-ADCPs do not work properly in estuaries because of sound inflection.

Although several methods are proposed to estimate velocity distribution (e.g. Chiu & Hsu, 2006; Maghrebi & Ball, 2006), results are disputable in complicated flow fields such as stratified tidal flows or unsteady flows. Thus, an innovative method and or equipment are required for continuous measurement of river discharge.

In the present study, Fluvial Acoustic Tomography (FAT) system is developed and utilized to measure flow rates in a tidal estuary. The FAT system have advantages in comparison to the competing techniques, namely accurate measurement of travel time by GPS clock, high signal-to-noise ratio due to 10^{th} order M-sequence modulation (Simon et al., 1985; Zheng et al., 1998). As a result, the FAT system works accurately even during flood events when SSC and sound noises are

very large. Moreover, the FAT system was tested successfully even in estuaries with frequent salt-water intrusions (Kawanisi et al., 2010).

2 MEASUREMENT PRINCIPLES AND ERROR ANALYSIS

The applied basic principle is similar to what is used in an acoustic velocimeter (AVM), in other words the cross-sectional averaged velocity is calculated by "time of travel method" (Sloat & Gain, 1995). The AVM measures an average velocity along a transverse line. Therefore, the AVM needs several strategies (index velocity method and velocity profile method) for computing discharge. In fact, the FAT system is able of estimating cross-sectional average velocity using multiple ray paths that cover whole section unlike the old-fashioned type of AVM. If measuring only one component of velocity field is supposed to be enough for a reliable flow rate calculation, the FAT system should be operated with only a couple of transducers. Otherwise a four-station system with two crossing transmission lines is required (e.g. for meandering rivers).

Let us consider two acoustic stations in a fluid medium moving with velocity $\mathbf{u}$. The travel time along the reciprocal ray path $\Gamma^{\pm}$ between a couple of transducers in the flowing medium is formulated as:

$$t_i^{\pm} = \int_{\Gamma_i^{\pm}} \frac{ds}{c(x,y) \pm \mathbf{u}(x,y) \cdot \mathbf{n}} \quad (i = 1, 2, ..., M) \tag{1}$$

where +/− represent the positive/negative direction from one transducer to another. c = the sound speed , ds = the increment of arc length measured along the ray, $\mathbf{u}$ = the water velocity, $\mathbf{n}$ = the unit vector along the ray and M = the number of rays. The path integrals are taken along rays. We assume that the two-way path geometry is reciprocal and $\Gamma_i^{\pm} \approx \Gamma_i$. The two-way travel time difference may be expressed as:

$$\begin{aligned} \Delta t_i &= \left(t_i^- - t_i^+\right) = \int_{\Gamma_i} \frac{2\mathbf{u} \cdot \mathbf{n}}{c^2 - (\mathbf{u} \cdot \mathbf{n})^2} ds \\ &\approx \int_{\Gamma_i} \frac{2\mathbf{u} \cdot \mathbf{n}}{c^2} ds \approx \frac{2L_i u_{mi}}{{c_{mi}}^2} \end{aligned} \tag{2}$$

where u_{mi} and c_{mi} are the range averaged water velocity and the sound speed along the ray path, respectively:

$$u_{mi} = \frac{1}{L_i} \int_{\Gamma_i} \mathbf{u} \cdot \mathbf{n} \; ds \tag{3}$$

$$c_{mi} = \frac{1}{L_i} \int_{\Gamma_i} c \; ds \tag{4}$$

where L_i = the length of ray path. The c_{mi} is calculated from

$$\begin{aligned} t_{mi} &= \frac{1}{2}\left(t_i^- + t_i^+\right) = \int_{\Gamma=i} \frac{c}{c^2 - (\mathbf{u} \cdot \mathbf{n})^2} ds \\ &\approx \int_{\Gamma_i} \frac{1}{c} ds = \frac{L_i}{c_{mi}} \end{aligned} \tag{5}$$

The velocity component in the direction of flow v_m is given by

$$\begin{aligned} v_m &= \frac{u_m}{\cos\theta} = \frac{1}{\cos\theta} \frac{1}{M} \sum_{i=1}^{M} u_{mi} \\ &= \frac{1}{\cos\theta} \frac{1}{2M} \sum_{i=1}^{M} \frac{{c_{mi}}^2}{L_i} \Delta t_i \end{aligned} \tag{6}$$

where u_m is mean velocity component along the ray paths, and θ the angle between the ray path and streamline.

In order to estimate the cross-sectional averaged velocity v_m, the ray pattern is preferable to cover the cross-section as much as possible. The ray paths of FAT system probably cover the cross-section in freshwater environment. However, developing a salt wedge under the transducer causes the ray paths to be reflected, so these ray paths won't be able to penetrate more into the bottom layers (Kawanisi et al., 2010).

By taking the total differentiation of Eqs. (5) and (6), the relative errors of c_m and u_m are estimated as Eqs. (7) and (8), respectively:

$$\frac{\delta c_m}{c_m} = \frac{\delta L}{L} - \frac{\delta t_m}{t_m} \tag{7}$$

$$\frac{\delta u_m}{u_m} = \frac{\delta L}{L} - 2\frac{\delta t_m}{t_m} + \frac{\delta(\Delta t_m)}{\Delta t} \tag{8}$$

The average travel time errors δt_m and $\delta(\Delta t)$ are negligible when both systems are synchronized precisely with GPS clock. As a result, the relative error of the average sound speed $\delta c_m / c_m$ and the relative error of the average velocity $\delta u_m / u_m$ are equated to the relative error of the horizontal distance $\delta L / L$. Concerning Eq. (8), the most right term is negligible only if the time accuracy is radiant, i.e. $\delta(\Delta t_m) / \Delta t$ is insignificant.

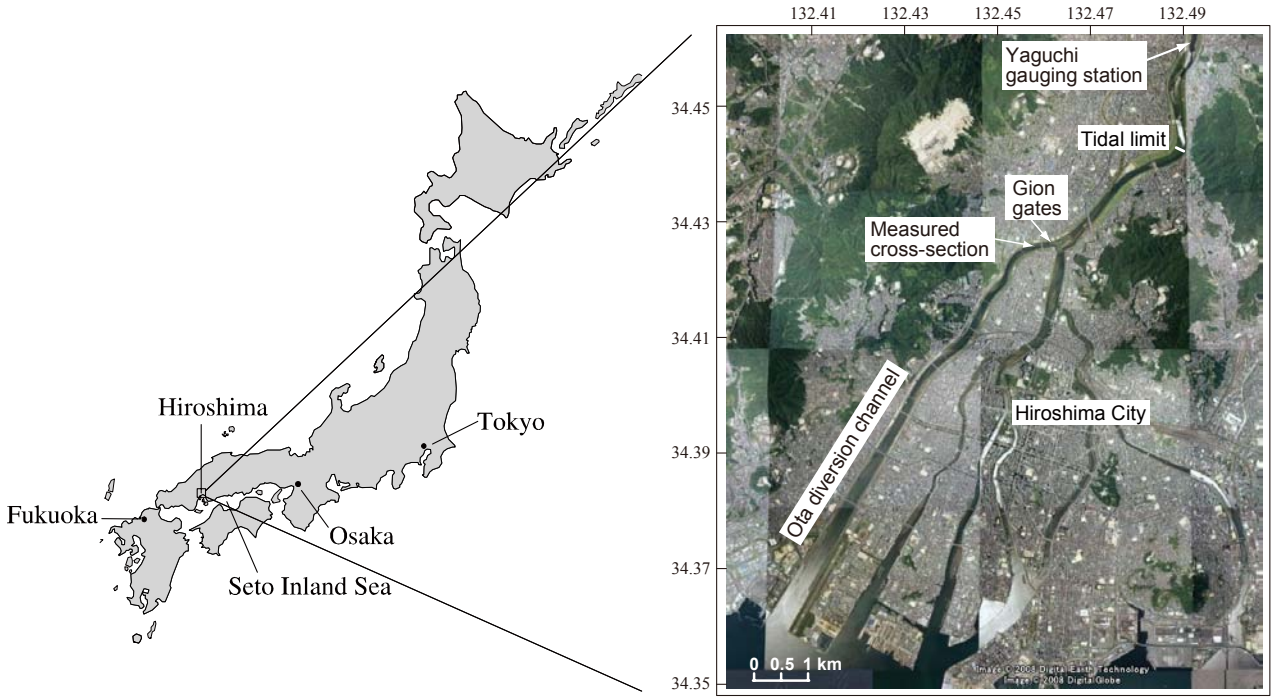

Figure 1. Study area and experimental site.

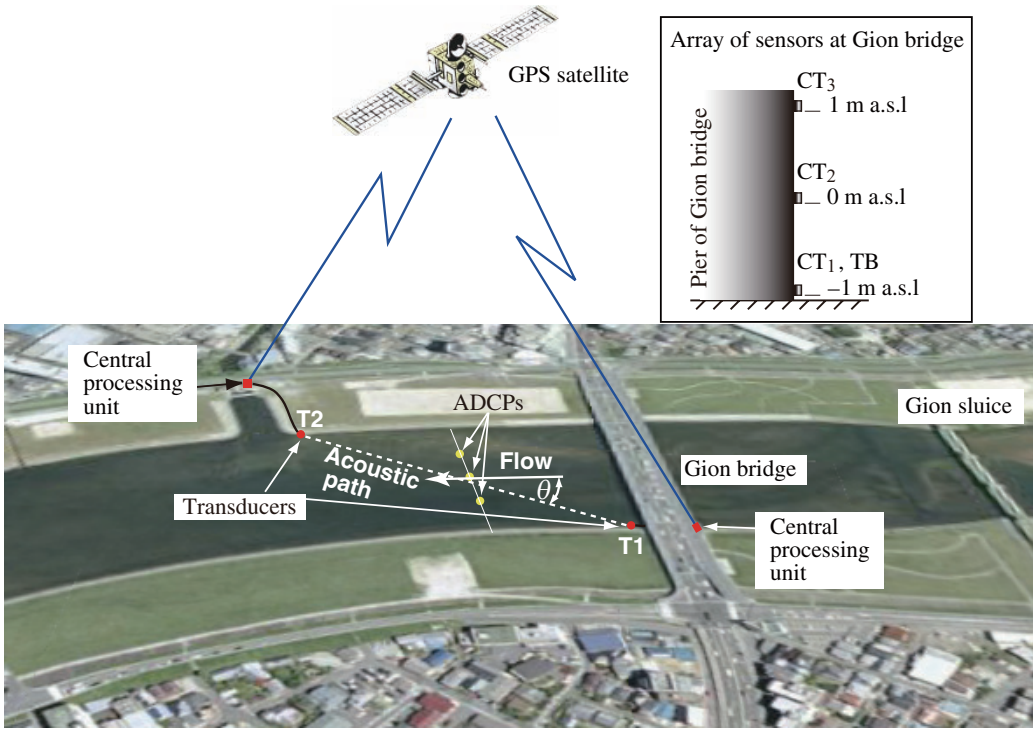

Figure 2. Aerial view of the experimental set-up.

3 EXPERIMENTAL SITE AND METHODOLOGY

3.1 *Study Area*

A FAT experiment was carried out during June through August 2009 in the Ota River, Japan. Figure 1 shows the aerial photograph of experimental site. The Ota River bifurcates into two main branches in about 9 km upstream from the mouth. The upstream border of tidal compartment in the Ota River estuary is located about 13 km upstream far from the mouth. The observation site was located 246 m downstream from the Gion sluice gates near the branched region (Fig. 1). The Ota diversion channel at the observation site is 120 m wide with a bed slope of about 0.04 %, and the water depth varies in a range from 0.3 m to 3 m depending on tidal phases.

The freshwater runoff into the diversion channel is usually controlled by the array of Gion sluice gates, located near the bifurcation

place. Usually only one sluice gate is opened slightly in order to make the stream cross-section of $32\,\mathrm{m}\times 0.3\,\mathrm{m}$ for spilling water. The inflow discharge is vaguely 10 ~ 20 % of the total flow rate of the Ota River in normal days. However, the accurate discharge at the Gion sluice gates is indefinite because the flow is influenced by tidal oscillation and saltwater intrusion. During flood events, all sluice gates are completely opened and the freshwater runoff from the Gion sluice gates is designed to be about half of the total river discharge. Since the flow at the Yaguchi gauging station that is located in 14 km upstream from the mouth, is not tidally modulated, the Ota River discharge before the bifurcation can be estimated from rating curves.

3.2 *Methodology*

A couple of broad-band transducers were installed diagonally across the channel as shown in Fig. 2. The FAT system simultaneously transmitted sound pulses from the omni-directional transducers every minute triggered by a GPS clock.

The streamwise velocity component v is estimated from the velocity component along the ray path u as $v = u/\cos\theta$. Other characteristics of the FAT system are listed as: (a) the central frequency of broad-band transducers is 30 kHz, (b) the angle between the ray path and stream direction θ is 30 degrees, (c) as shown in Fig. 3, the transducers were mounted at 0.2 m heigh above the bottom, the altitudes of upstream and downstream transducers are $-0.46\pm0.01\,\mathrm{m}$ a.s.l (above the mean sea level) and -0.7 ± 0.01 m a.s.l, respectively.

Three moored ADCPs (Aquadopp profiler, Nortek AS) are employed to validate the discharge data obtained from the FAT system. As shown in Fig. 2, the ADCPs are arranged at 30 m transverse intervals with the central ADCP put at the river centerline.

The bin length is set to 0.1 m, the interval of ensemble average to 120 s, and the profiling interval to 300 s. The accuracy of horizontal velocity is as small as 0.028 m/s. The blank zone of ADCP measurement near the water surface is 0.22 m in thickness while that near the bottom is estimated by $d(1-\cos 25^\circ)+0.1\,\mathrm{m}$, where d is the distance from the ADCP transducer level to the river bed.

Water level and vertical distribution of temperature and salinity are measured every 10 minutes by the conductivity-temperature (C-T) sensors, attached to the pier of the Gion Bridge at 40 m from the left bank (Fig. 2). The cross-sectional distribution of temperature and salinity is measured by the successive CTD casts from the Gion Bridge. Transverse spacing of CTD casts is set to 20 m and it takes about 10 minutes to complete the traverse.

The channel bathymetry along the transmission line was surveyed (with an accuracy of 0.01 m) on 17 March 2008. The result can be found in Fig. 3 as the river cross-sections.

3.3 *Ray tracing simulation*

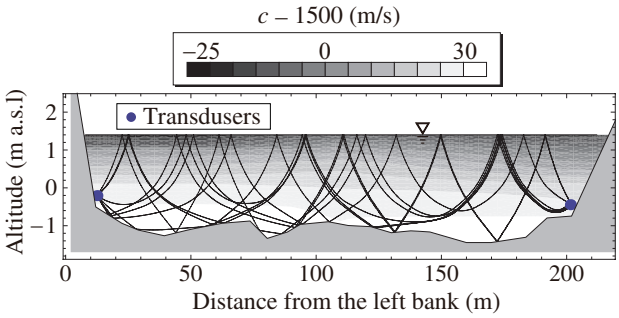

Figure 3. Example of river cross-section, contour plots of sound speed distribution and the result of ray simulation (ray pattern).

In order to estimate the cross-sectional average velocity, sound paths are expected to traverse a larger stream section between the bottom and surface. If the sound speed has an inhomogeneous distribution in the section, sound rays draw curves obeying Snell's law of refraction. In this paper, ray simulation is implemented by solving the following differential equations (Dushaw & Colosi, 1998):

$$\begin{aligned}\frac{d\varphi}{dr} &= \frac{\partial c}{\partial r}\frac{1}{c}\tan\varphi - \frac{\partial c}{\partial z}\frac{1}{c}\\ \frac{dz}{dr} &= \tan\varphi\\ \frac{dt}{dr} &= \frac{\sec\varphi}{c}\end{aligned} \tag{9}$$

where φ is the angle of ray measured from the horizontal axis r, $z=$ vertical coordinate, and $t=$ time. Here, the sound speed c is estimated by Medwin's formula (Eq. 10) that is a function of temperature T (°C), salinity S, and depth D (m) (Medwin, 1975):

$$\begin{aligned}c = {} & 1449.2 + 4.6T - 0.055T^2 + 2.9\times10^{-4}T^3\\ & + (1.34 - 0.01T)(S-35) + 0.016D\end{aligned} \tag{10}$$

Notice that we do not need to notify [psu] as the salinity unit, since the practical salinity adopted by the UNESCO/ICES/SCOR/IAPSO Joint Panel on Oceanographic Tables and Standards have any dimensions. In the ray simulation, effect of

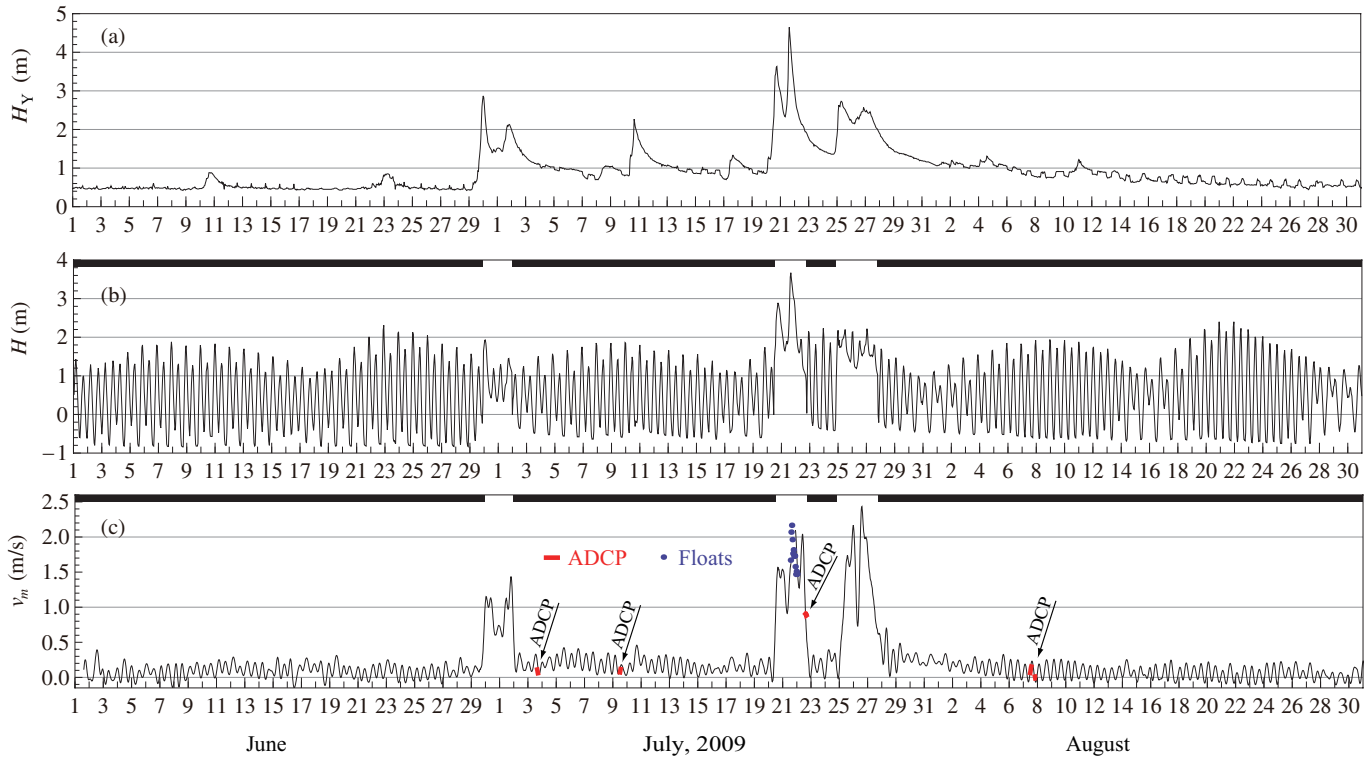

Figure 4. Time plots of water level at Yaguchi (a) and Gion (b), and cross-sectional average velocity (c) for three months.

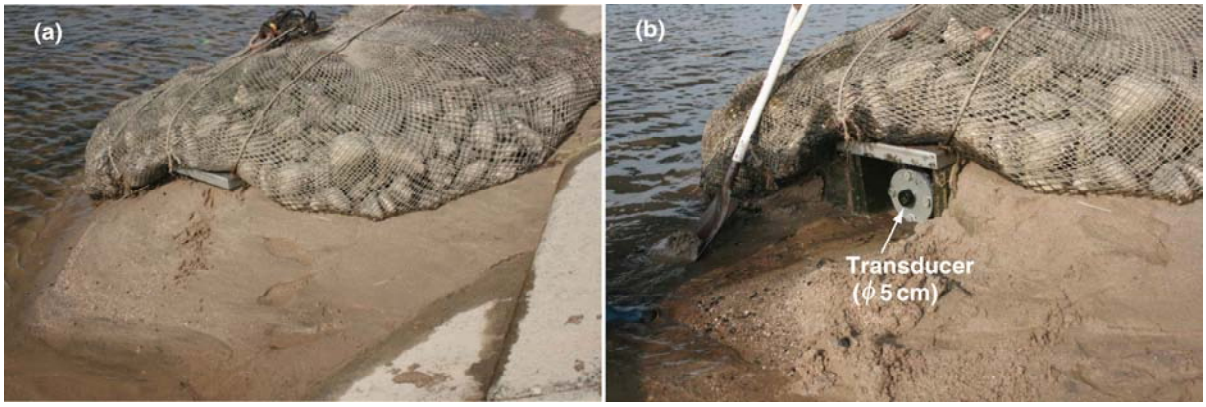

Figure 5. (a) Sand sedimentation on the left transducer induced by the flood event, (b) the left transducer after removing the sand.

velocity is negligible compared to that of sound speed.

4 RESULTS AND DISCUSSION

4.1 *Ray pattern*

In general, the cross-section of a river can be deemed as a wave guide. Fig. 3 shows the typical ray pattern in the cross-section of low-water channel, drawn on the grey color map of sound speed. The rays with bottom reflection numbers greater than five are not shown in Fig. 3. They correspond to rays released at larger angles from the horizontal at the source position.

Mostly, the ray paths can cross approximately all the section as illustrated in Fig. 3. Unfortunately, in a short period (before and after LWS) of near-bed salt wedge intrusion, the sound rays emitted in the upper layer were reflected at the underlying interface and prevented from penetration into lower layers (Kawanisi et al., 2010). In this case, the cross- sectional average velocity is overestimated by the FAT system since it cannot cover all the cross sections. The water discharge is roughly overestimated by 10 % on average in the particular period of limited freshwater discharge (Kawanisi et al., 2010). Since there is not a salt wedge during flood events, the rays can cover all the cross sections. Accordingly no correction for the cross-sectional average velocity is needed

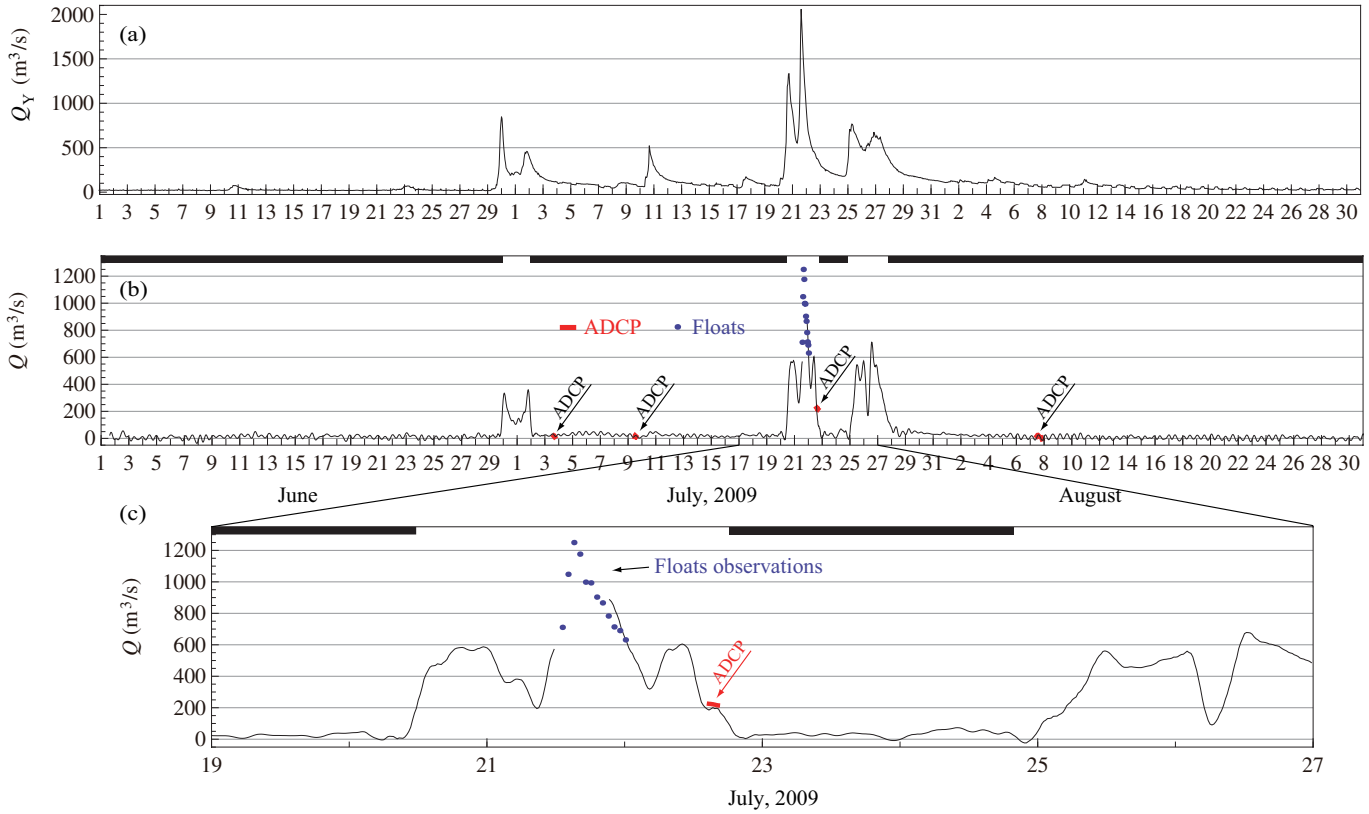

Figure 6. Time plots of discharge at Yaguchi (a) and Gion (b) for three months; Gion discharge for 19-27th July (c).

4.2 *Temporal variation of cross-sectional average velocity and water discharge*

The cross-sectional average velocity v_m is calculated by the following formula:

$$v_m = u_m / \cos\theta \tag{11}$$

where $\theta =$ the angle between the ray path projection to the horizontal plane and streamlines. The cross-sectional average velocity measured by the FAT system is compared to that of arrayed ADCPs and the floats observations in Fig. 4 (c). Fig. 4 (a) and (b) show water level variations at the Yaguchi and Gion gauging stations,respectively. The upper solid bars in Fig.4 (b) and (c) indicate that the Gion sluices are in regular position The ADCP data fall over the cross-sectional average velocity measured by the FAT system. Unfortunately, FAT system did not work well around the flood event peak on July 21, because of sand sedimentation over the left transducer as shown in Fig. 5. However, the floats data serve to interpolate the period of data lacking in the FAT data.

The velocity variation in the observation site is usually dominated by semi-diurnal and diurnal tidal components and also disturbed significantly by unknown factors, caused by discharge control of the Gion sluice gates to reduce inflow into the observation site.

Water discharge is calculated by the following formula:

$$Q = A(H)v_m \sin\theta = A(H)u_m \tan\theta \tag{12}$$

where $A(H) =$ cross-sectional area, spanned by ray paths. The three-month variations of the Yaguchi discharge estimated by rating curves and flow discharge by FAT system are shown in Figs. 6 (a) and (b). Figure 6 (c) indicates the discharge at the Gion during the largest flood event for comparing the FAT and the float data. The discharge measured by the FAT system is compared with the arrayed ADCP and floats results in this figure as well.

Three methods of measuring discharge show almost the same results. Thus, Fig. 6 supports that the discharge obtained from the FAT system is close to the actual river discharge.

As illustrated above, FAT system measurement was unsuccessful because the left transducer was covered with sand. However, the discharge estimated by the FAT system is meaningless when the water surface is over the flood plain ($H > 3$m) because FAT system measures only the discharge across the low-water channel compartment. All the presented data are in $H < 3$m. Therefore, the comparisons between the FAT and float data in Fig. 6 (c) have a meaningful aspect. It is found that the both flow rates are concurrent while the FAT system works properly.

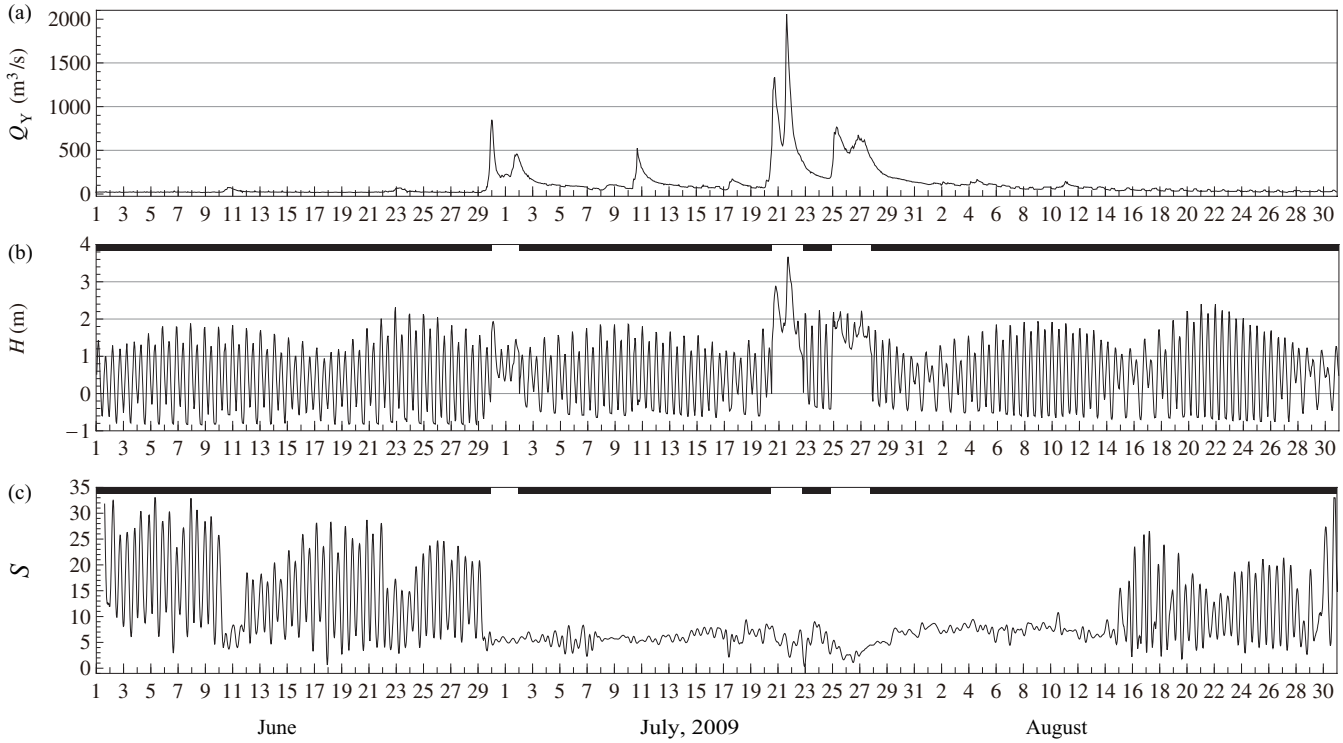

Figure 7. Time plots of discharge at Yaguchi (a), water level at Gion (b), and cross-sectional average salinity (c) for three months.

It is no wonder that the Gion discharge Q correlates with the Yaguchi discharge Q_Y. However, the discharge ratio Q/Q_Y changes significantly even when all sluice gates are completely opened: $Q/Q_Y \approx 0.4 \sim 0.9$.

From the results in Figs. 4 and 6, the long-term measurement of cross-sectional average velocity and river discharge is successfully fulfilled by the FAT system even in an estuary with salt wedge intrusion and flood events. It is, thus, suggested that the present FAT system is a prospective method for the continuous measurement of river discharge.

4.3 *Temporal variation of cross-sectional average salinity*

The cross-sectional average salinity measured by the FAT system is presented together with the Yaguchi discharge and the Gion water level in Fig. 7. It is noticeable that the salinity dominantly changes during the observation period. The cross-sectional average salinity is deduced from the sound speed data of FAT system and the water temperature at the Gion Bridge, using Eq. (10). It is should be noted that using temperature may cause certain quantity of error in salinity estimations because the Gion Bridge temperature can be different from the average temperature along the cross-section of the FAT system. However, the error is probably insignificant for the following qualitative discussion.

Obviously, there are tidal driven salinity variations while the freshwater inflow is limited by the Gion sluice gates. It is found that the mean salinity is sensitive to the Yaguchi discharge even when the Gion gates are in their regular position.

The salinity drastically decreases by the first flood event (the first opening of the Gion gates) and the saltwater intrusion cannot be found until the middle of August. Moreover, it is remarkable that the saltwater intrusion is strengthened during the neap tide and the re-intrusion of saltwater to the experimental site is sparked by the small tidal range. Conversely, the spring tides depress the saltwater intrusions.

5 CONCLUSIONS

The fluvial acoustic tomography (FAT) system, characterized by the GPS precise clock system and the M-sequence modulation of transmission signals was developed and applied to a shallow tidal river with saltwater intrusion. The FAT system is composed of a couple of acoustic transducers, located on both sides of a channel and sound transmission line between them is arranged at an angle of about 30 degrees to the channel axis in order to make the measurement of the cross-sectional average velocity efficient.

The signal-to-noise ratio of the received signals was remarkably improved by the signal transmission, phase-modulated by the 10th order

M-sequence. The FAT system is asserted as a powerful tool to measure river discharge even under flood events with high turbidity concentration and large ambient noise levels of sound.

The long-term measurement of the cross-sectional average velocity and river discharge were carried out successfully in spite of the periodic intrusion of a salt wedge into the river and a large amount of suspended/bed load. It is concluded that the fluvial acoustic tomography (FAT) is a prospective method for the continuous monitoring of tidal river discharge.

The cross-sectional average velocity of the river stream was estimated from the travel time difference data (obtained along the sound paths) acquired in the low-water channel cross-section. Moreover, the cross-sectional average salinity is able to be estimated using the FAT data such as sound speed data, ray simulation results and the temperature data by the C-T sensors. This suggests that the freshwater discharge in tidal rivers can also be determined by the FAT system after separating the salt water component.

ACKNOLDGEMENTS

We would like to thank Dr. Noriaki Gohda of Hiroshima University/Aqua Environmental Monitoring Limited Liability Partnership (AEM-LLP) for the strong support in field works and data processing. This study is supported by a fund from “the Construction Technology Research and Development Program of the Ministry of Land, Infrastructure, Transport and Tourism of Japan”, and “the River Fund”.

REFERENCES

Catherine, A. R. and DeRose J. B. 2004. Investigation of hydroacoustic flow-monitoring alternatives at the Sacramento river at Freeport, California: Results of the 2002-2004 pilot study. Scientific Investigation Report, USGS.

Chiu, C. L. and Hsu S. M. 2006. Probabilistic approach to modeling of velocity distributions in fluid flows. Journal of Hydrology, 316, 28-42.

Dushaw, B.D. and Colosi, J.A. 1998. Ray tracing for ocean acoustic tomography. Technical Memorandum, Applied Physics Laboratory, University of Washington, (TM 3-98): 31 pp.

Kawanisi, K., Razaz, M., Kaneko, A. and Watanabe S. 2009. Long-term mea-surement of stream flow and salinity in a tidal river by the use of the fluvial acoustic tomography system. Journal of Hydrology, 380(1-2), 74-81; DOI: 10.1016/j.jhydrol.2009.10.024.

Maghrebi, M. F. and Ball, J. F. 2006. New method for estimation of discharge. Journal of Hydraulic Engineering, ASCE, 132(10), 1044-1015.

Medwin, H. 1975. Speed of sound in water: A simple equation for realistic para-meters. Journal Acoustical Society of America, 58, 1318-1319.

Sloat, J. V. and Gain W. S. 1995. Application of acoustic velocity meters for gaging discharge of three low-velocity tidal streams in the St. John River Basin, Northeast Florida. U.S. Geological Survey, Water-Resources Investi-gations Report, 95-4230, 26.

Simon, M. K., Omura, J. K. and Levitt, B. K., 1985. Spread Spectrum Communications Handbook. McGraw-Hill, New York, 423 pp.

Wang, F. and Huang H. 2005. Horizontal acoustic Doppler current profiler (H-ADCP) for real-time open channel flow measurement: flow calculation model and field validation. Proc. XXXI IAHR CONGRESS, 319-328.

Zheng, H., H. Yamaoka, N. Gohda, H. Noguchi and A. Kaneko 1998. Design of the acoustic tomography system for velocity measurement with an application to the coastal sea, J. Acoust. Soc. Japan (E), 19, 199-210.